Zeitschrift für Kristallographie, Bd. 117, S. 331–343 (1962)

Determination and refinement of the crystal structure of bustamite, $CaMnSi_2O_6$

By **Donald R. Peacor** and **M. J. Buerger**

Massachusetts Institute of Technology, Cambridge, Massachusetts

With 8 figures

(Received July 8, 1962)

Auszug

Bustamit ist triklin; in der Raumgruppe $F\bar{1}$ mit $a = 15{,}412$ Å, $b = 7{,}157$ Å, $c = 13{,}824$ Å, $\alpha = 89°29'$, $\beta = 94°51'$, $\gamma = 102°56'$ enthält die Zelle 12 $CaMnSi_2O_6$. Dreidimensionale Interferenzdaten wurden mit dem Einkristall-Diffraktometer gewonnen. Die Anwendung der Minimumfunktion auf $P(xz)$ und der Vergleich der Elementarzellen von Bustamit und Wollastonit führte zu einem Strukturvorschlag, der nach der Ausgleichsmethode verfeinert wurde.

Nahezu dichtest gepackte Ebenen von O-Atomen verlaufen parallel (101). Zwischen diesen Ebenen liegen abwechselnd Ebenen aus Si-Atomen in tetraedrischer Koordination und Ebenen, die Ca- und Mg-Atome in oktaedrischer Koordination geordnet enthalten. Die Tetraeder um Si sind zu Ketten parallel der b-Achse verbunden, mit einer Identitätsperiode von drei Tetraedern.

Abstract

Bustamite is triclinic, space group $F\bar{1}$, with cell dimensions $a = 15.412$ Å, $b = 7.157$ Å, $c = 13.824$ Å, $\alpha = 89°29'$, $\beta = 94°51'$, $\gamma = 102°56'$. The unit cell ideally contains $12(CaMnSi_2O_6)$. Three-dimensional intensity data were gathered with the single-crystal Geiger-counter diffractometer. Application of the minimum function to $P(xz)$, and comparison of the unit cells of bustamite and wollastonite yielded a trial structure which was refined with least-squares.

Planes of approximately close-packed oxygen atoms are oriented parallel to (101). Planes containing Ca and Mn atoms in octahedral coordination alternate with planes of Si atoms in tetrahedral coordination between oxygen planes. Ca and Mn are ordered. Si tetrahedra are linked to form chains parallel to b with a repeat unit of three tetrahedra.

Introduction

Several authors have noted the similarity of the properties of bustamite, $CaMnSi_2O_6$, to those of wollastonite, $CaSiO_3$. On the basis

Table 1. *Symmetry and unit-cell data for bustamite and wollastonite*

Space group	Wollastonite (BUERGER[5]) $P\bar{1}$	Bustamite (BERMAN and GONYER[4]) $P1$ or $P\bar{1}$	Bustamite (BUERGER[5]) $F\bar{1}$	β $Mn_{0,8}Ca_{0,2}SiO_3$ (LIEBAU *et al.*[6]) $F1$ or $F\bar{1}$	Bustamite (PEACOR and BUERGER) $F\bar{1}$
a	7.94 Å	7.64 Å	2×7.73 Å	2×8.03 Å	15.412 Å
b	7.32	7.16	7.18	7.11	7.157
c	7.07	6.87	2×6.92	2×6.84	13.824
α	90°02′	92°08′	89°34′	—	89°29′
β	95°22′	94°54½′	94°53′	—	94°51′
γ	103°26′	101°35′	102°47′	—	102°56′

of a similarity of optical properties of the two minerals, SUNDIUS[1] and SCHALLER[2,3] proposed that bustamite is Mn-rich wollastonite. BERMAN and GONYER[4] accepted this view when they determined the unit cell of bustamite and noted its correspondence to that of wollastonite (Table 1). BUERGER[5] and LIEBAU *et al.*[6] found, however, that the unit cells are different although closely related (Table 1).

Because of the recent interest in the structures of the minerals of the wollastonite family, it is important to understand the relation of bustamite to other triclinic metasilicates. In this paper the results of an investigation of the structure are given.

Unit cell and space group

Specimens of bustamite from Franklin, N. J., were kindly provided by Professor C. FRONDEL of Harvard University. The unit cell obtained

[1] N. SUNDIUS, On the triclinic manganiferous pyroxenes. Amer. Mineral. **16** (1931) 411–429, 488–518.

[2] WALDEMAR T. SCHALLER, Johannsenite, a new manganese pyroxene. Amer. Mineral. **23** (1938) 575–582.

[3] WALDEMAR T. SCHALLER, The pectolite–schizolite–serandite series. Amer. Mineral. **40** (1955) 1022–1031.

[4] H. BERMAN and F. A. GONYER. The structural lattice and classification of bustamite. Amer. Mineral. **22** (1937) 215–216.

[5] M. J. BUERGER, The arrangement of atoms in crystals of the wollastonite group of metasilicates. Proc. Nat. Acad. Sci. **42** (1956) 113–116.

[6] F. LIEBAU, M. SPRUNG and E. THILO, Über das System $MnSiO_3$–$CaMn(SiO_3)_2$. Z. anorg. allg. Chem. **297** (1958) 213–225.

diffractometer with the b axis as rotation axis. Intensities of the reflections with Cu$K\alpha$ radiation were measured with an argon-filled Geiger counter. Care was taken not to exceed the linearity range of the Geiger counter; counting rates were maintained below 500 c.p.s. by using aluminum absorption foils. Intensities were measured by direct counting. Background was measured on each side of a peak and the average background subtracted from the value of background plus integrated intensity obtained by scanning through the peak. Of approximately 1650 non-equivalent reflections in the Cu sphere, 1212 were recorded. These were corrected for the Lorentz and polarization factors using an IBM 709 program written by C. T. PREWITT[9], and for absorption using an IBM 709 program written by C. W. BURNHAM[10].

Structure determination

Determination of x and z coordinates. Comparison of $h0l$ reflections of bustamite and wollastonite showed that the distribution and intensities of each were similar. This suggested that the projections of the structures along b are the same. The Patterson projection $P(xz)$ of bustamite was therefore prepared. Its similarity to that of $P(xz)$ of wollastonite confirmed that the structures are very probably the same in projection.

The structure of wollastonite[11] projected along b is shown in Fig. 1. Ca_1 and Ca_2 are superimposed in projection. On the assumption that Ca and Mn atoms in bustamite have a similar arrangement, a minimum function $M_2(xz)$ was prepared for bustamite using the equivalent of the superimposed $Ca_1 + Ca_2$ inversion peaks of wollastonite. In wollastonite, the Patterson projection $P(xz)$ contains an image of the structure as seen from Ca_3. The Patterson projection and $M_2(xz)$ were therefore superimposed to obtain the minimum function $M_4(xz)$ shown in Fig. 2.

Note that for each atom of $\varrho(xz)$ there is a corresponding peak of the correct relative weight in $M_4(xz)$ of bustamite. There are four extra peaks, labelled A, B, C, and D, in $M_4(xz)$. Three of these, A, B,

---

[9] C. T. PREWITT, The parameters Υ and φ for equi-inclination, with application to the single-crystal counter diffractometer. Z. Kristallogr. **114** (1961) 355–360.

[10] C. W. BURNHAM. The structures and crystal chemistry of the aluminum-silicate minerals. Ph. D. Thesis (1961) M. I. T.

[11] M. J. BUERGER and C. T. PREWITT. The crystal structures of wollastonite and pectolite. Proc. Nat. Acad. Sci. **47** (1961) 1884–1888.

and C, are near the peaks corresponding to O_7, O_8 and Si_3 of wollastonite. Structure factors F_{h0l}, calculated omitting these atoms, gave a discrepancy factor $R = 31\%$. Using these structure factors the electron-density projections $\varrho(xz)$, Fig. 3, and $\Delta\varrho(xz)$ were then calculated. As can be seen from a comparison of Figs. 1 and 3, these

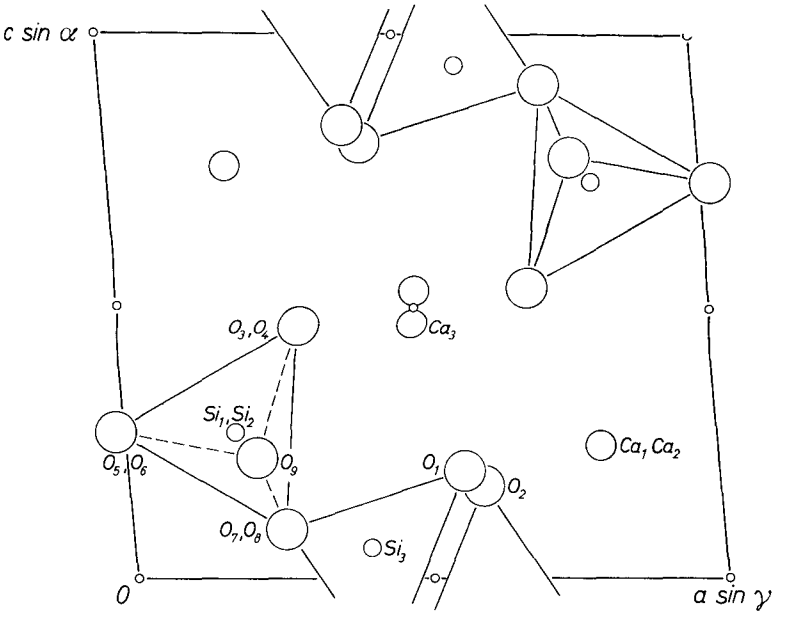

Fig. 1. Projection along b of the structure of wollastonite. Oxygen atoms are represented by large circles, Ca atoms by circles of intermediate size, and Si atoms by small circles.

confirmed that the projections $\varrho(xz)$ of bustamite and wollastonite are essentially the same. None of the false peaks, A, B, C and D of $M_4(xz)$ appeared in $\varrho(xz)$, while peaks corresponding to O_7, O_8 and Si_3 do occur. A second structure-factor calculation based on coordinates from $\varrho(xz)$ and $\Delta\varrho(xz)$ yielded an R of 21% for all F_{h0l}.

Determination of y coordinates. The lower part of Fig. 4 shows the primitive triclinic unit cell of wollastonite and the upper part shows the face-centered bustamite cell in corresponding orientation. Inversion centers coinciding with lattice points are shown as solid circles and all other inversion centers as open circles. All inversion centers lie on (101) planes which intersect a and c at 0 and $\frac{1}{2}$ in wollastonite and at 0, $\frac{1}{4}$, $\frac{1}{2}$ and $\frac{3}{4}$ in bustamite. The distribution of inversion centers is the same in both structures, except that those centers on planes

parallel to (101) in bustamite intersecting a and c at $\frac{1}{4}$ and a and c at $\frac{3}{4}$ are shifted by $\frac{b}{4}$ relative to those in wollastonite.

Figures 1 and 3 show that Si and (Ca, Mn) atoms lie approximately on planes parallel to (101) which contain the inversion centers in both

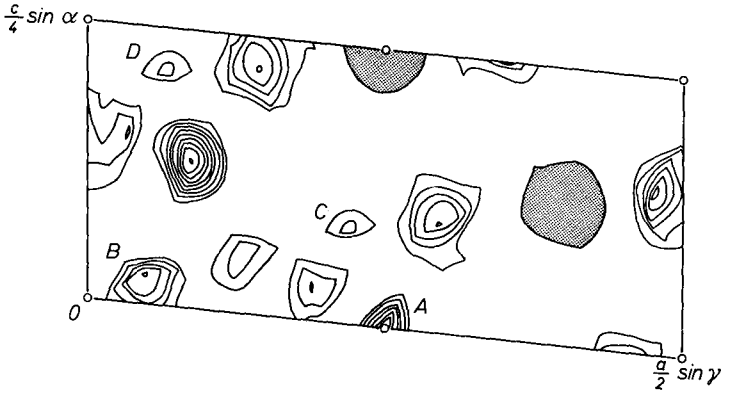

Fig. 2. Bustamite, $M_4(xz)$. The high (Ca + Mn) peaks are shaded. Peaks which do not correspond to atoms are labelled A, B, C, and D.

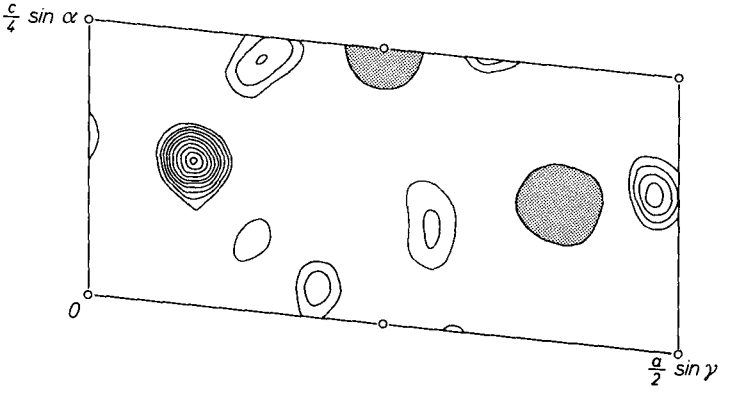

Fig. 3. Bustamite, $\varrho(xz)$. (Ca + Mn) peaks are shaded.

structures. Planes containing Si atoms alternate with those containing (Ca, Mn).

Figure 1 shows that in wollastonite there are inversion centers in the (101) planes at $y = 0$ and $\frac{1}{2}$. Because the substructure has period $\frac{b}{2}$, there are also pseudocenters for the Ca atoms and their coordinating oxygen atoms, which project at the same xz coordinates, at $y = \frac{1}{4}$ and $\frac{3}{4}$. Since the Si atoms are not in the substructure these pseudocenters do not apply to them.

A reasonable model for the structure of bustamite results from combining the above information with the fact that wollastonite and bustamite are similar in projection. Coordinates of Ca and Mn atoms and their coordinating oxygen atoms in bustamite differ from those in wollastonite in the following ways:

1. The pseudoinversion centers in wollastonite at $y = \frac{1}{4}, \frac{3}{4}$ in (101) planes containing Ca become true inversion centers in bustamite.

2. The inversion centers at $y = 0, \frac{1}{2}$ in wollastonite become pseudoinversion centers in bustamite.

The relative arrangement of silica tetrahedra is the same in both structures except that tetrahedra in alternating sheets are displaced by $\frac{b}{2}$ by the face-centering translation in bustamite.

The above arrangement of inversion centers requires that the (Ca, Mn) of bustamite, equivalent to Ca_3 of wollastonite, be located on inversion centers; that is, four (Ca, Mn) atoms are still in two general positions of rank 2, and two (Ca, Mn) atoms are on centers with rank 1. This is just the distribution required for ordering of Ca and Mn atoms which was noted in the section on unit cell and space group.

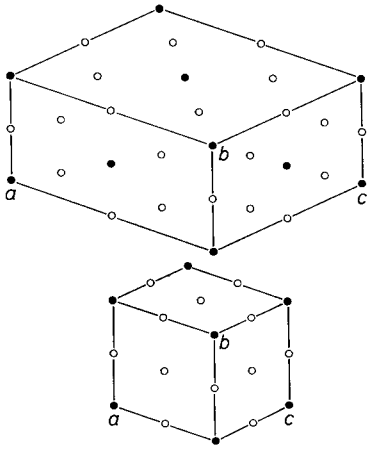

Fig. 4. Comparison of the unit cells of bustamite (above) and wollastonite (below). Lattice points (which are coincident with inversion centers) are shown as solid circles. Other inversion centers are shown as open circles.

Structure factors were calculated for all 1212 observed reflections using x and z parameters derived from the projection, and y parameters of wollastonite adjusted as required above. Ca and Mn atoms were assumed to be completely disordered, since at this point there was still no direct evidence for ordering. The discrepancy factor, R, was only 31%, suggesting that the proposed structure was probably correct.

Refinement

Refinement was carried out using SFLSQ2, a least-squares IBM 709 program using the full matrix[12]. For the initial refinement, form-factor curves were used for Ca and Mn assuming complete disorder,

and a correction made for the average real component of anomalous dispersion. All atoms were assumed to be half ionized. All 1212 reflections were used as input to each cycle of refinement, but those reflections with $(F_o - F_c)/F_c > 0.5$ were rejected by the program. The weighting scheme recommended by HUGHES[13] was used throughout. Isotropic temperature factors for all atoms were initially set at 0.5, a value consistent with temperature factors of other silicate structures refined in this laboratory.

The discrepancy factor R decreased to 12.3% after only three cycles, confirming the correctness of the proposed structure. For these cycles, only the scale factor and coordinates were allowed to vary.

Table 2. *Interatomic distances and cation peak heights after cycle 3 of refinement*

Cation number	Equipoint rank	Average cation-oxygen interatomic distance	Peak height in $\Delta\varrho$ (xyz)	Interpretation of ordering
1	2	2.25 Å	377	Mn, excess Ca
2	2	2.38	−1170	Ca
3	1	2.21	642	Mn
4	1	2.39	−1250	Ca

Using structure factors calculated from coordinates of cycle 3, a three-dimensional difference Fourier synthesis $\Delta\varrho(xyz)$ was computed. (All three-dimensional Fourier syntheses were computed using the IBM 709/7090 program ERFR2[14]). The only major discontinuities in the synthesis were negative or positive peaks at the positions of (Ca + Mn) atoms. The peak heights are listed in Table 2. Interatomic distances, also shown in Table 2, were calculated using ORXFE, an IBM 704 program[15].

Mn has five more electrons than Ca, assuming equal ionization of Mn and Ca. Thus the positive peaks at the positions of cations 1 and 3 clearly indicate that Mn atoms are located there, while the negative peaks of cations 2 and 4 suggest that Ca occupies those positions.

[12] C. T. PREWITT, SFLSQ2, an IBM 7090 program for least-squares refinement. (Unpublished).

[13] E. W. HUGHES, The crystal structure of melamine. J. Amer. Chem. Soc. **63** (1941) 1737–1752.

[14] W. G. SLY, D. P. SHOEMAKER and J. H. VAN DER HENDE, ERFR2, IBM 790/7090 Fourier program. (Unpublished).

[15] W. R. BUSING and H. A. LEVY, A crystallographic function and error program for the IBM 704. Oak Ridge National Laboratory Report No. 59–12–3, 1959.

The radius of Mn^{+2} (0.91 Å) is less than that of Ca^{+2} (1.06Å). The smaller average cation-oxygen distances of cations 1 and 3 and the larger distances of cations 2 and 4 therefore confirm the ordering indicated by the peaks of $\Delta\varrho(xyz)$.

It was noted above that there is an excess of Ca over Mn in the material used for this study. The peak at the position of cation 1 in $\Delta\varrho(xyz)$ is slightly lower than that for cation 3. In addition, the average cation-oxygen distance is slightly larger for cation 1 than for cation 3. This indicates that the excess Ca substitutes for Mn preferentially in the site labelled cation 1.

Table 3. *Coordinates and isotropic temperature factors for atoms of bustamite*

	x	$\sigma(x)$	y	$\sigma(y)$	z	$\sigma(z)$	B	$\sigma(B)$
Mn_1	.1009	.0001	.6725	.0003	.3733	.0001	.56	.03
Ca_1	.0994	.0001	.1583	.0004	.3785	.0001	.69	.03
Mn_2	$\frac{1}{4}$	0	0	0	$\frac{1}{4}$	0	.56	.04
Ca_2	$\frac{1}{4}$	0	$\frac{1}{2}$	0	$\frac{1}{4}$	0	.73	.05
Si_1	.0884	.0002	.2003	.0005	.1343	.0002	.34	.04
Si_2	.0888	.0002	.6454	.0005	.1325	.0002	.32	.04
Si_3	.1975	.0002	.9805	.0005	.0218	.0002	.16	.04
O_1	.2158	.0005	.9758	.0014	.4027	.0005	.68	.12
O_2	.2018	.0005	.4840	.0014	.4069	.0005	.57	.12
O_3	.1563	.0005	.1838	.0014	.2293	.0005	.48	.12
O_4	.1509	.0005	.7206	.0014	.2315	.0005	.50	.12
O_5	.0131	.0005	.3964	.0014	.3549	.0005	.64	.12
O_6	.0140	.0005	.8513	.0014	.3717	.0005	.66	.12
O_7	.1287	.0005	.1240	.0014	.0393	.0005	.57	.12
O_8	.1364	.0005	.7625	.0013	.0411	.0005	.29	.11
O_9	.0926	.0006	.4250	.0016	.1147	.0006	1.34	.14

Three structure-factor computations were made (taking account of both the real and imaginary components of anomalous dispersion of Mn and Ca) for the following distributions of the excess Ca:

1. all excess Ca assigned to cation 1;
2. $\frac{1}{3}$ excess Ca assigned to cation 1, $\frac{2}{3}$ to cation 3;
3. all excess Ca assigned to cation 3.

The R value was essentially equal for all three distributions ($\sim 9.5\%$) but the comparison of F_{obs} and F_{cal} was slightly better with the excess Ca substituting for the Mn of cation 1. Since this confirmed the conclusion reached on the basis of the peaks of $\Delta\varrho(xyz)$ and the interatomic distances, this distribution of the excess Ca was accepted as being correct.

Refinement was continued with the Ca and Mn distribution determined above, taking full account of anomalous dispersion. The Zn, Fe and Mg reported in the analysis were considered to substitute for Mn, since these atoms are smaller than Mn.

Two more cycles (4 and 5) were executed varying only coordinates and the scale factor. The coordinates were essentially unchanged in cycle 5. Individual isotropic temperature factors were varied in cycles 6 and 7. Refinement was concluded with two cycles, in the first of which the coordinates and the scale factor were permitted to vary, and another cycle in which isotropic temperature factors were refined. Final parameters and their errors are listed in Table 3.

Description of the bustamite structure

The electron density $\varrho(xyz)$ was computed using the signs of the structure factors of the final cycle of refinement. The peaks of this three-dimensional function are shown projected parallel to b in Fig. 5.

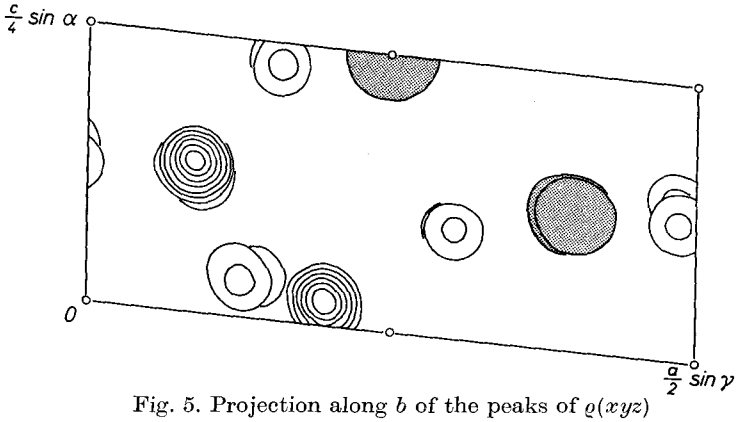

Fig. 5. Projection along b of the peaks of $\varrho(xyz)$

Figure 6 is an interpretation of the same projection. The similarity of the structures of bustamite and wollastonite (Fig. 1) has been noted above several times. The relations between these structures is discussed in another place[16].

In Fig. 6 the arrangement of oxygen atoms crudely approximates close packing, all oxygen atoms except O_9 lying in sheets which are parallel to (101). Ca and Mn atoms and Si atoms alternate in layers between sheets of oxygen atoms, with Ca and Mn in octahedral coordination and Si in tetrahedral coordination. SiO_4 tetrahedra all share two oxygen atoms with other tetrahedra to form a chain whose repeat

[16] D. R. PEACOR and C. T. PREWITT, Comparison of the crystal structures of bustamite andwollastonite. Amer. Mineral. (In press.)

unit is three tetrahedra and which is oriented parallel to the b axis. The nature of the arrangement of tetrahedra is best shown in Figs. 7 and 8. Figure 7 is a projection of the structure parallel to a while Fig. 8 is a projection along c.

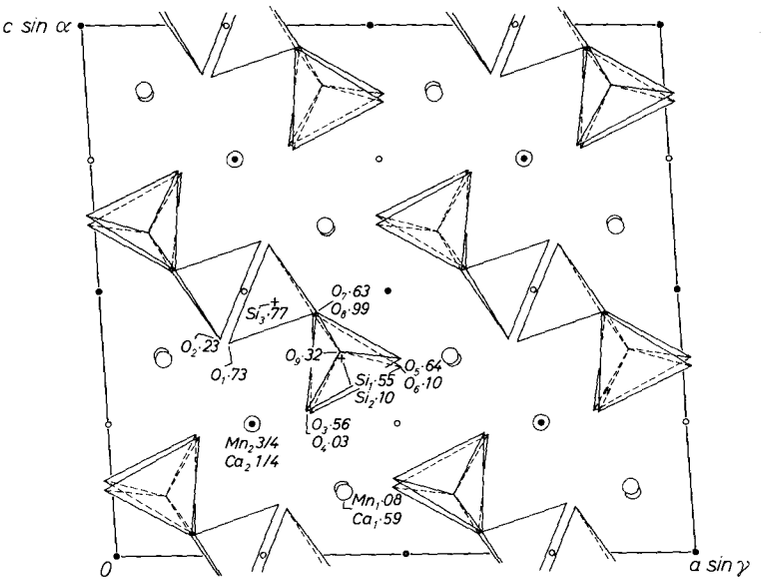

Fig. 6. Interpretation of $\varrho(xyz)$. Inversion centers at $y = 0,\frac{1}{2}$ shown as solid circles, and inversion centers at $y = \frac{1}{4},\frac{3}{4}$ as open circles.

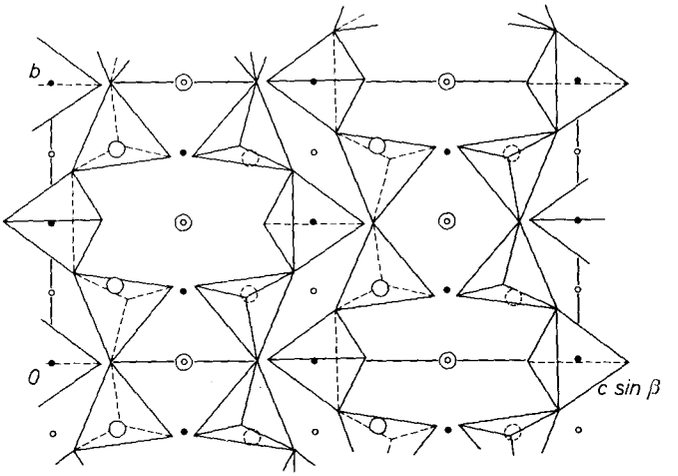

Fig. 7. Structure of bustamite from $x = \frac{1}{4}$ to $-\frac{1}{4}$ projected onto a plane defined by the axes b and $c \sin \beta$.

The sheet of Ca and Mn octahedra can be compared to the sheet of Mg octahedra in brucite. Octahedra share edges to form a continuous two-dimensional sheet in brucite. The wollastonite arrangement may be interpreted in terms of ideal close packing of the oxygen atoms in sheets coordinating Ca atoms. As shown in Figs. 7 and 8, octahedra share edges to form a band three octahedra wide, extending infinitely

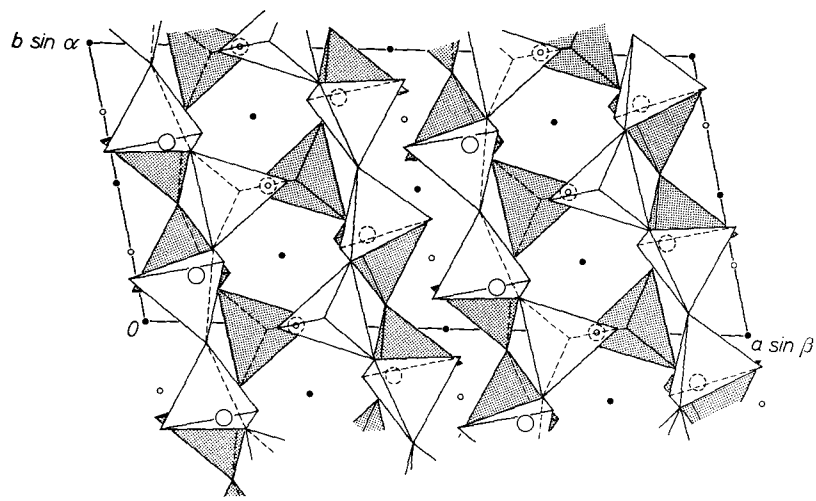

Fig. 8. Projection along c of the structure of bustamite

parallel to b. Individual bands are separated by a column of unoccupied octahedrally coordinated voids. There is actually considerable distortion of the close-packed oxygen layers, however, particularly around the column of vacant octahedra.

Interatomic distances are listed in Table 4. These are discussed in detail elsewhere[16]. All distances are close to accepted values. The average Si—O distance is 1.623 Å. SMITH and BAILEY[17] state that the average Si—O distance of a silicate is a function of the extent of tetrahedral linkage. The distance 1.623 Å falls exactly at the value predicted by them for metasilicates.

There are three non-equivalent Si—O—Si angles in bustamite, which are:

$$\begin{aligned} Si_1—O_9—Si_2 \quad & 161°, \\ Si_1—O_7—Si_4 \quad & 135°, \\ Si_2—O_8—Si_4 \quad & 137°. \end{aligned}$$

[17] J. V. SMITH and S. W. BAILEY, Second review of Al—O and Si—O tetrahedral distances. Acta Crystallogr. (In press).

Corresponding angles in wollastonite are 149°, 139° and 140° respectively[18]. In a survey of Si—O—Si angles, LIEBAU[19] found that the average for well-determined structures is about 140°. Angles greater than 150° are uncommon and, under normal conditions, represent a

Table 4. *Interatomic distances in bustamite*

Si_1—O_3	1.628 Å	Ca_1—O_1	2.437 Å	Mn_2—$2O_1$	2.215
O_5	1.587	O_2	2.531	$2O_3$	2.154
O_7	1.645	O_3	2.298	$2O_4$	2.241
O_9	1.616	O_5	2.382	Average	2.203
Average	1.619	O_6	2.302		
		O_8	2.358	Ca_2—$2O_2$	2.344
Si_2—O_4	1.626	O_9	2.899	$2O_3$	2.412
O_6	1.585	Average	2.384	$2O_4$	2.421
O_8	1.647	(excluding O_9)		$2O_9$	2.891
O_9	1.613			Average	2.392
Average	1.618	Mn_1—O_1	2.499	(excluding O_9)	
		O_2	2.286		
Si_3—O_1	1.600	O_4	2.163		
O_2	1.595	O_5	2.144		
O_7	1.660	O_6	2.041		
O_8	1.671	O_7	2.335		
Average	1.632	Average	2.245		

relatively unstable condition. The angle Si_1—O_9—Si_2 is large in both bustamite and wollastonite, but unusually so in bustamite. In addition, the isotropic temperature factor for O_9 of bustamite is considerably larger (1.34) than all other temperature factors of the structure (see Table 3). In wollastonite, this temperature factor (0.68) is only slightly above the average for the entire structure.

Acknowledgements

This work was supported by a grant from the National Science Foundation. Calculations were performed in part on the IBM 7090 computer at the M. I. T. Computation Center.

[18] C. T. PREWITT and M. J. BUERGER, A comparison of the crystal structures of wollastonite and pectolite. (In press).

[19] FRIEDRICH LIEBAU, Untersuchungen über die Größe des Si—O—Si-Valenzwinkels. Acta Crystallogr. **14** (1961) 1103—1109.